Journal of Geophysical Research: Oceans

RESEARCH ARTICLE
10.1029/2017JC013708

Storm Impact on Morphological Evolution of a Sandy Inlet

Julia Hopkins[1], **Steve Elgar**[2], **and Britt Raubenheimer**[2]

[1]Delft University of Technology, Delft, Netherlands, [2]Woods Hole Oceanographic Institution, Woods Hole, MA, USA

Key Points:
- SWAN+Delft3D-FLOW model agrees with observations of hurricane waves, currents, and morphological change
- Bathymetric change is correlated with storm intensity (total storm energy divided by duration) in a mixed wave-and-tidal-current system
- Short, intense hurricanes can cause more sediment transport than longer, less intense nor'easters with the same time-integrated energy

Correspondence to:
J. Hopkins,
j.a.hopkins@tudelft.nl

Citation:
Hopkins, J., Elgar, S., & Raubenheimer, B. (2018). Storm impact on morphological evolution of a sandy inlet. *Journal of Geophysical Research: Oceans*, *123*, 5751–5762. https://doi.org/10.1029/2017JC013708

Received 17 DEC 2017
Accepted 12 JUL 2018
Accepted article online 23 JUL 2018
Published online 18 AUG 2018

Abstract Observations of waves, currents, and bathymetric change in shallow water (<10-m depth) both inside and offshore of a migrating inlet with strong (2–3 m/s) tidal currents and complex nearshore bathymetry show over 2.5 m of erosion and accretion resulting from each of two hurricanes (offshore wave heights >8 m). A numerical model (Delft3D, 2DH mode) simulating waves, currents, and morphological change reproduces the observations with the inclusion of hurricane force winds and sediment transport parameters adjusted based on model-data comparisons. For simulations of short hurricanes and longer nor'easters with identical offshore total time-integrated wave energy, but different peak wave energies and storm durations, morphological change is correlated (R^2 = 0.60) with storm intensity (total energy of the storm divided by the duration of the storm). Similarly, the erosion observed at the Sand Engine in the Netherlands is correlated with storm intensity. The observations and simulations suggest that the temporal distribution of energy in a storm event, as well as the total energy, impacts subsequent nearshore morphological change. Increased storm intensity enhances sediment transport in bathymetrically complex, mixed wave-and-tidal-current energy environments, as well as at other wave-dominated sandy beaches.

Plain Language Summary This study uses field observations and numerical simulations to understand the impact of storm events on coastal areas. We focus on complex coastal environments, here a tidal inlet, where the shoreline is constantly moving owing to a combination of strong waves and strong tidal currents. Numerical simulations, verified with field observations during Hurricane Irene and Hurricane Sandy, allow us to test how storm intensity impacts sediment transport in this complex area. Storms with high intensity are short-lived, but have high waves (hurricanes), while storms with low intensity are longer but with lower waves at the peak (nor'easters). Simulations suggest that high-intensity storms cause more erosion than low-intensity storms even with identical storm energy.

1. Introduction

Accurate predictions of changes in nearshore bathymetry are necessary for managing beaches, ports, and coastal infrastructure, as well as for planning resilient nearshore communities. Changes in nearshore bathymetry are pronounced during storms, when high-energy waves, wave-driven flows, and storm surge can alter the shoreface of a beach in just days or even hours (Herrling & Winter, 2014; Lindemer et al., 2010; Miller, 1999; and many others). On decadal time scales, long-term observations of changes in shallow bathymetry along barrier islands in the Gulf of Mexico (Morton et al., 1995; Wahl & Plant, 2015) and the East Coast of the United States (Hapke et al., 2016; Moore et al., 2013) suggest that storm events correlate with the evolution of the coastline, with sea level rise becoming more important on time scales of centuries (Ruggiero et al., 2010). Additionally, the enhanced shoreline changes observed in 2013 at beaches in Europe, relative to changes observed during the previous decade, correlated with unusually energetic storm waves (Masselink et al., 2016).

Hydrodynamic simulations of storm conditions from coupled wave and current models compare well with observations of hurricane waves and storm surge along barrier islands and offshore of estuaries (Dietrich et al., 2011; Lindemer et al., 2010; Mulligan et al., 2010; and many others). Further, coupled hydrodynamic and morphodynamic models have been used in wave-dominated environments to simulate the observed subaerial response of relatively long straight beaches to hurricanes (Dissanayake et al., 2014; Harter & Figlus, 2017; Lindemer et al., 2010; Smallegan et al., 2016). Simulations of multiple storms on wave-dominated sandy beaches suggest that bathymetric change scales with wave energy and that storm direction can influence patterns of erosion and deposition (Luijendijk et al., 2017; Walstra et al., 2012).

Here these previous results are extended using observations of hurricane-induced subaqueous (<10-m water depth) bathymetric change along a sandy shoreline with a migrating inlet. Unlike many previous studies on

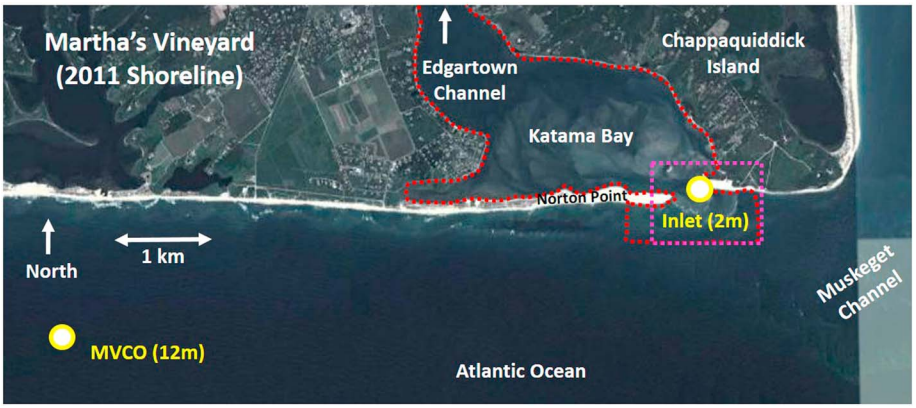

Figure 1. Satellite image of Martha's Vineyard in 2011. White circles with yellow outlines indicate locations of wave (MVCO, bottom left) and current (Inlet, middle right) sensors deployed during Hurricanes Irene and Sandy. The red dotted curve surrounds the area surveyed before and after Hurricane Irene (similar for Sandy). The pink dotted box encompasses the area in which sediment transport (e.g., erosion and accretion) is calculated. MVCO = Martha's Vineyard Coastal Observatory.

wave-dominated beaches, strong tidal currents in the inlet and in the nearshore may contribute significantly to sediment transport.

The field observations are used to calibrate a numerical model that simulates nearshore hydrodynamics, sediment transport, and morphological change along the southern shoreline of Martha's Vineyard, MA (Figure 1; Hopkins et al., 2016, 2017). Norton Point, the sand barrier separating Katama Bay from the Atlantic Ocean, breached during a nor'easter storm in April 2007 to form Katama Inlet (Figure 1). The inlet migrated 2.5 km eastward until it closed in 2015 (Hopkins et al., 2017; Orescanin et al., 2016). Between 2011 and 2015, tidal currents observed in Katama Inlet were as high as 2 m/s (Orescanin et al., 2016) and tidal currents flowing through Muskeget Channel separating Vineyard Sound from the Atlantic (Figure 1) were as high as 3 m/s (Hopkins et al., 2017). Observations at this site were used in prior studies to calibrate and validate the numerical model Delft3D (Lesser et al., 2004) for waves and currents (Hopkins et al., 2016, 2017). Here rapid morphological evolution and associated waves and currents observed at Katama are used to calibrate Delft3D for sediment transport. The model is applied to investigate the effects on nearshore subaqueous sediment transport of short, highly energetic (e.g., hurricanes) and longer, less energetic (e.g., nor'easters) storms.

2. Observations

Simulations of measured bathymetric change focus on Hurricanes Irene and Sandy, two of the most energetic storms to affect the East Coast of the United States in the last few decades. In 2011, Irene produced storm surge up to 1.2 m in the Northeast (Avila & Cangialosi, 2011), and in 2012, Sandy caused inundation of over 1.8 m in similar areas (Blake et al., 2013).

To investigate the impact of these storms on Katama, bathymetry from the northern end of Edgartown Channel (connecting Katama Bay to Vineyard Sound, north of the arrow in Figure 1) through Katama Bay and Inlet and across the ebb shoal in the ocean to the south (Figure 1, red dotted curve) was measured with a GPS- and acoustic-altimeter-equipped personal watercraft. The vertical resolution of the surveys is approximately 0.05 m, and the horizontal resolution is 0.10 m along transects separated by 5 (around regions of complex bathymetry) to 60 m (uniform bathymetry). Surveys were conducted before (6 August 2011) and after (30 August 2011) the passage of Hurricane Irene (28–29 August 2011) and before (2 October 2012) and after (11 November 2012) the passage of Hurricane Sandy (30 October 2012) and a nor'easter (7–9 November 2012). The bay surface area is approximately 7.5×10^6 m^2, and water depths range from less than 1 m on the flood shoal to 10 m at the northern part of the bay (Orescanin et al., 2016).

Offshore waves measured in ~50-m depth with NOAA buoy 44097 ranged from 0.5 to 9.5 m. Waves in 12-m depth were measured at the Martha's Vineyard Coastal Observatory (MVCO, http://www.whoi.edu/mvco), and currents in Katama Inlet were measured with an acoustic Doppler velocimeter with a sample volume

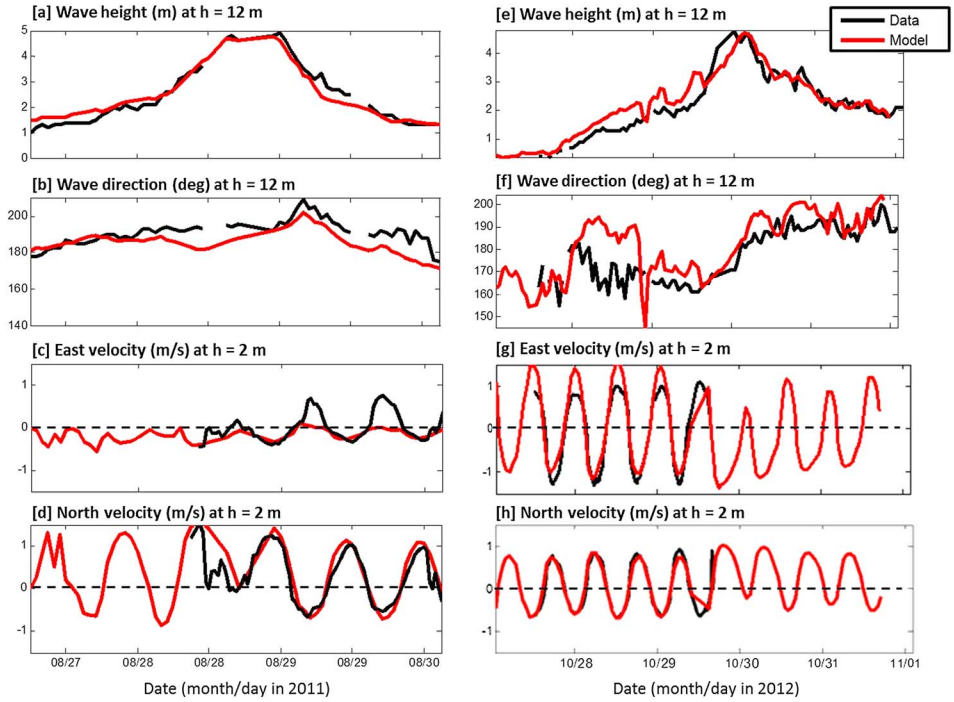

Figure 2. Observed (black curves) and modeled (red curves) (a, e) significant wave height and (b, f) wave direction at MVCO (12-m depth), and (c, g) east-west and (d, h) north-south velocity inside the inlet mouth (~2-m depth) for Hurricanes (a–d) Irene and (e–h) Sandy.

about 0.8 m above the sandy seafloor in ~2-m depth (Figures 1 and 2). Bottom pressures were corrected for atmospheric pressure fluctuations and converted to sea surface elevation fluctuations assuming hydrostatic pressure and using the linear dispersion relationship (Dean & Dalrymple, 1991).

3. Numerical Simulations

Waves and currents were simulated with the numerical models SWAN (Booij et al., 1999) and Delft3D-FLOW (in 2DH mode, Lesser et al., 2004), respectively. The wave model solves the spectral action balance and includes the effects of shoaling, refraction, and wave-current interaction. The circulation model includes the effects of waves on currents through wave radiation-stress gradients, combined wave and current bed shear stress, and Stokes drift. The wave and flow models were coupled such that FLOW passes water levels and Eulerian depth-averaged velocities to SWAN and SWAN passes wave parameters to FLOW.

SWAN was run with 36 10°-wide directional bins and 37 frequency bands logarithmically spaced between 0.03 and 1.00 Hz. The model also used a depth-limited wave breaking formulation without rollers (Battjes & Janssen, 1978), with the default value $\gamma = H_{sig}/h = 0.73$ (where the significant wave height H_{sig} is 4 times the standard deviation of sea surface elevation fluctuations, and h is the water depth), and a JONSWAP bottom friction coefficient associated with wave-orbital motions set to 0.10 m^2/s^3 (Hopkins et al., 2016).

The circulation model was run using the 13 most energetic satellite-generated tidal constituents (Egbert & Erofeeva, 2002) along open boundaries, which were dominated by the M2 (~80% of the variance, with small variation along the boundary) and N2 (~10% of the variance) constituents. In addition, the model used a free slip condition at closed (land) side boundaries, a spatially uniform Chezy roughness of 65 $m^{0.5}/s$ (roughly equivalent to a drag coefficient of $C_d = 0.0023$) at bottom boundaries, and default Delft3D parameters for coupling the FLOW and WAVE models (Deltares, 2014). Second-order differences were used with a time step of 0.15 s for numerical stability.

The wave model offshore boundary conditions are given by output from the WaveWatch3 (WW3) model (Tolman, 2002). Results are similar if offshore wave boundary conditions are given by the 50-m-depth buoy observations. During hurricanes, wind forcing within the model domain becomes important for accurate

simulations (see the appendix). Wind boundary data were acquired from WW3 (forced by the Global Data Assimilation Scheme; Tolman, 2002), consistent with the WW3 wave boundary data.

Sediment transport (Van Rijn, 1993) was simulated using the modeled waves and currents. Model parameters were set to default values with a grain size of 500 μm (based on sediment cores taken around the inlet and bay both in 2013 and in previous studies; Anderson, 2012), except for the reference height (0.5 m), the current-related reference concentration factor (0.25), and the wave-related suspended and bed-load transport factors (0.1), which were reduced from the default values (1) that smoothed all bedforms and produced unrealistic transport around the island.

SWAN and Delft3D-FLOW (in depth-averaged mode) were run over four nested grids with both two-way (FLOW) and one-way nesting (SWAN). The outermost grid, with 1-km resolution, spans about 150 km along the north and south boundaries and 100 km along the east and west boundaries. Nested in this coarse grid are finer grids of 200-, 40-, and 13-m resolution (Hopkins et al., 2016). Large-scale bathymetry within the model domain was obtained during 1998 and 2008 USGS surveys (Northeast Atlantic 3-arc second map, National Geophysical Data Center, 1999, and Nantucket 1/3-arc second map, Eakins et al., 2009) and has horizontal resolution of 10 to 90 m. The large-scale bathymetry and the high-resolution bathymetry near the inlet were combined on a triangular mesh of variable resolution (finest (10-m spacing) near the inlet and coarsest (90-m spacing) in 12-m water depth), and subsequently interpolated onto each computational grid.

4. Results

4.1. Validation of Hydrodynamics

The SWAN-Delft3D wave and circulation model simulates accurately the wave heights, wave directions, and currents observed in 12-, 7-, and 2-m water depth (Hopkins et al., 2016), as well as the currents ranging from 0 to 2 m/s and flow structures observed from near the shoreline to the center of Muskeget Channel (Figure 1; Hopkins et al., 2017). Here using the WW3 wind and wave boundary conditions, simulated wave heights and directions agree with the observed wave heights (Figures 2a and 2e) and directions (Figures 2b and 2f) in 12-m depth water during both storm events. The model also simulates the currents observed in the inlet channel in approximately 2-m water depth (Figures 2c, 2d, 2g, and 2h). Some of the discrepancies in the simulated east current during Irene (Figure 2c) may be owing to spatially varying currents within the inlet that change on scales smaller than a model grid cell, especially near the observations in complex shallow bathymetry.

4.2. Validation of Morphodynamics

A wide range of metrics for model morphodynamic skill can be examined depending on the sediment transport quantities of interest, although interpreting these metrics often requires site-specific knowledge (Daly et al., 2014; Ganju et al., 2011; Luijendijk et al., 2017; Sutherland et al., 2004; and many others). Here qualitative metrics are used to give a sense of model skill on a case-by-case basis during storms. An accompanying quantitative model validation is given in the appendix.

The Delft3D numerical model results agree with the observed bathymetric changes owing to Hurricanes Irene and Sandy. Simulated spatial patterns and amplitudes of erosion and accretion (Figures 3b and 3d) are similar to those observed (Figures 3a and 3c). Further, the simulated bathymetric changes across and along the inlet, along the ebb shoal, and south of the inlet are consistent with the changes observed during the storms (cf. red with black curves in Figure 4). Some of the simulated patterns in erosion and accretion are shifted spatially relative to the observed patterns (Figure 4), possibly owing to artifacts associated with stretching and compressing different model prestorm and poststorm survey grids to align with larger-area surveys outside of the inlet region (see the appendix). Thus, although the magnitude and pattern of the simulated bathymetric change is consistent with the observed bathymetric change, the patterns are offset spatially by up to 50 m (Figure 4; see the appendix). The comparisons of the simulations with observations of hydrodynamics (Figure 2) and morphodynamics (Figures 3 and 4) suggest that the field-calibrated model can be used to study morphological evolution near Katama Inlet.

4.3. Storm Intensity Impact on Morphology

Alongshore sediment transport can be scaled roughly with the wave energy incident on a shoreline, and thus, episodic, high-wave events such as nor'easters and hurricanes shape the morphological evolution of wave

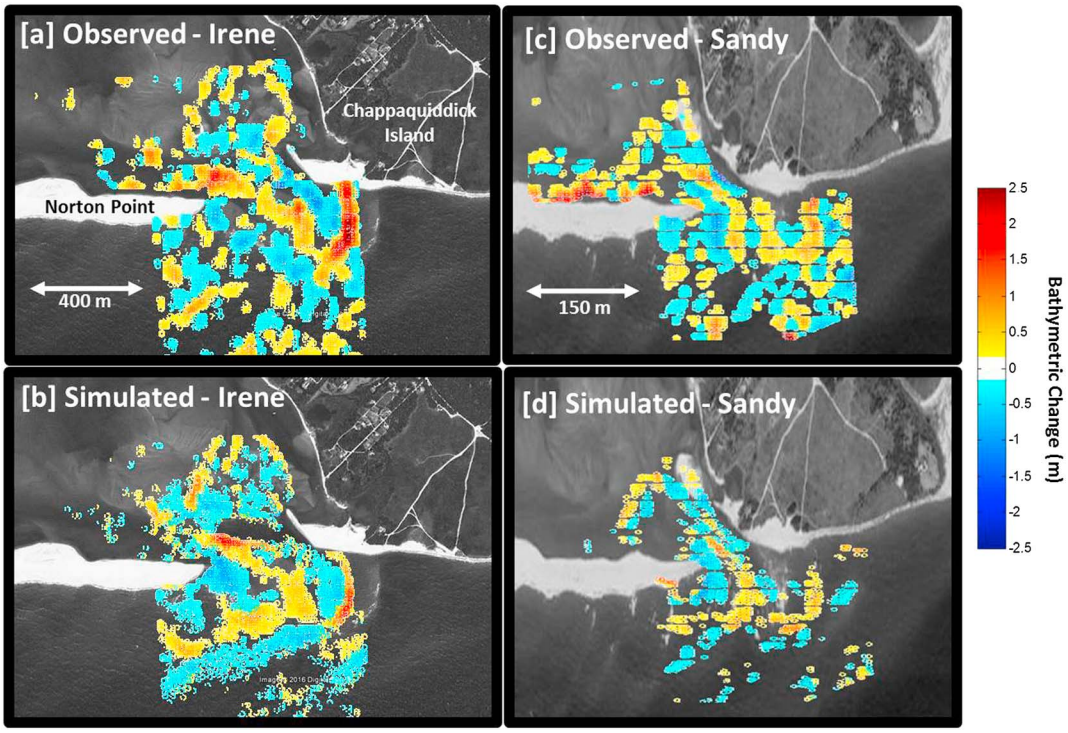

Figure 3. Bathymetric change (red is accretion, blue is erosion, scale on the right) for (a, c) observed and (b, d) simulated hurricane conditions for Hurricanes (a, b) Irene in 2011 and (c, d) Sandy in 2012. The observed prestorm and poststorm bathymetries are interpolated onto the 13-m horizontal spacing model grid. Changes less than 0.2 m are not shown.

energy-dominated nearshore environments (Herrling & Winter, 2014; Kaji et al., 2014; Walstra et al., 2013; and many others). The effect of episodic events on mixed wave-and-current energy systems is less well known, although recent studies at the Sand Engine in the Netherlands suggest that storm energy has a similar relationship to sediment transport in the presence of relatively weak tidal currents (<1 m/s) (Luijendijk et al., 2017) when wave-driven currents in the nearshore approach 1 m/s (Radermacher et al., 2017). Tidal currents observed near Katama (~3 m/s around the corner of Chappaquiddick Island and ~2 m/s through the inlet) can be stronger than those observed at the Sand Engine (0.8 m/s), and wave-driven currents tend to be weaker owing to smaller wave angles relative to the shoreline orientation (typically 1 m/s at the Sand Engine compared with 0.2 to 0.9 m/s south of Katama Bay, depending on wave energy and direction). Here the field-verified Delft3D wave-current-sediment transport model is used to determine the relative effects of short, intense storms (e.g., hurricanes) and longer, less intense storms (e.g., nor'easters) in the mixed wave-and-current energy Katama Inlet system.

For these idealized model simulations of storm events, the wave boundary conditions were based on observations at the 50-m water depth waverider buoy collected during Hurricane Irene. The offshore boundary significant wave height was modified to change the distribution of energy for Irene over time, while keeping constant the time-integrated storm energy (proportional to wave height squared) (Figure 5a). JONSWAP spectra at the boundary were generated based on the temporal distribution of offshore wave energy and a range of peak periods and offshore wave directions (Figures 5b and 5c). To ensure identical numbers of tidal cycles and tidal-current transport, all model runs were 6-days long regardless of the length of the storm peak.

Storm intensity was calculated in 12-m depth (to account for wave transformation over shallow offshore bathymetry) by integrating the energy of the storm under its peak (where wave heights are greater than 70% of the maximum height) and dividing by the duration of the storm peak. The erosion integrated over an area near the inlet (pink box in Figure 1, in which there was ~10% loss of sediment during the storm) after the 6 days is used to quantify the effect of storm intensity on nearshore sediment transport. The variance in bathymetric change and cumulative erosion and deposition have similar trends (not shown).

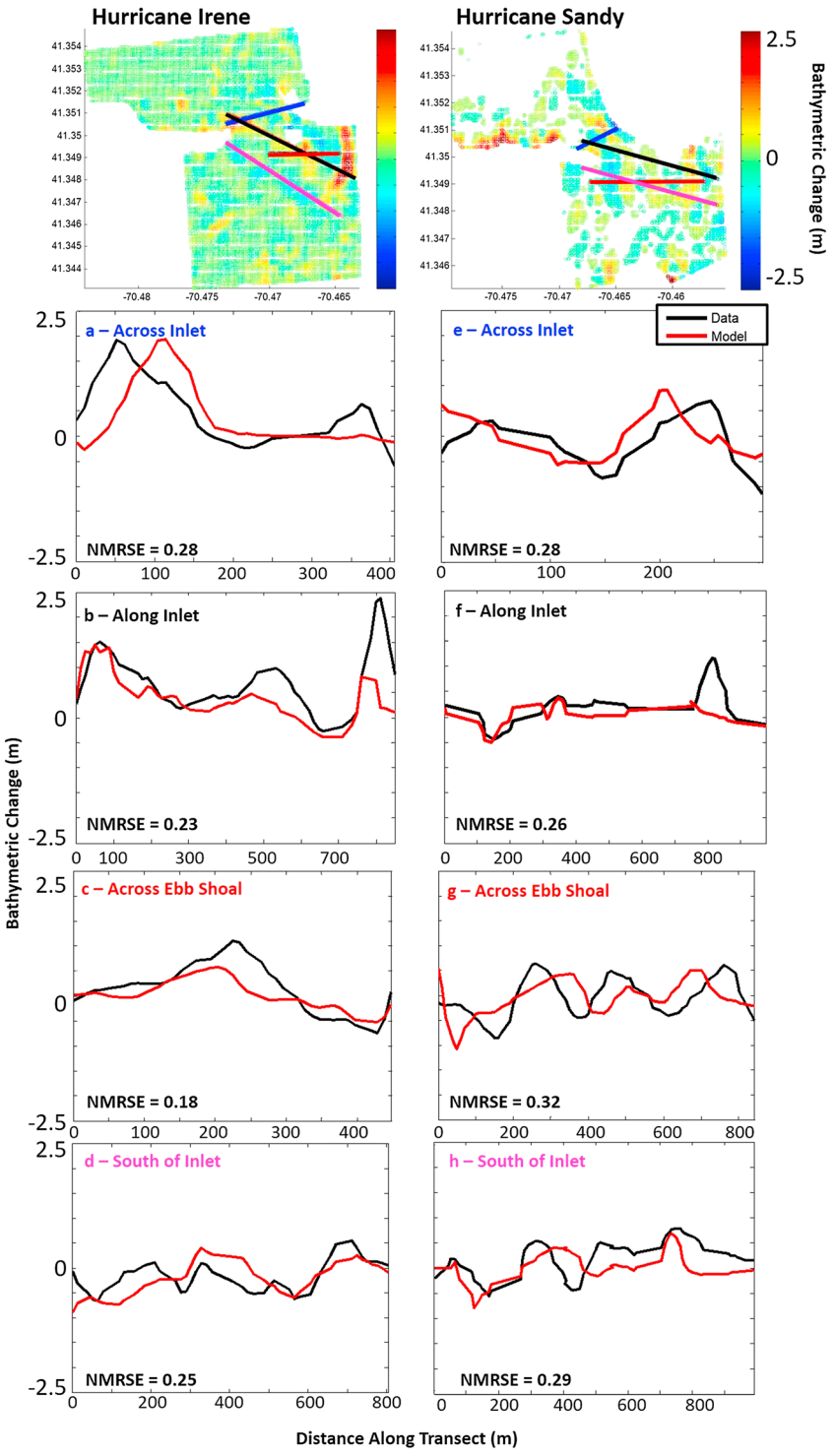

Figure 4. Observed (black curves) and simulated (red curves) erosion and accretion versus distance along transects located (a, e) across the inlet mouth (blue), (b, f) along the inlet channel (black), (c, g) across the ebb shoal (red), and (d, h) south of the inlet on the southern shoreline of Norton Point. The location of each transect is shown in the color contour plots of bathymetric change (top) for Hurricanes (left) Irene and (right) Sandy. The normalized root-mean-square error (NRMSE) for each comparison is listed in the lower left of the panels.

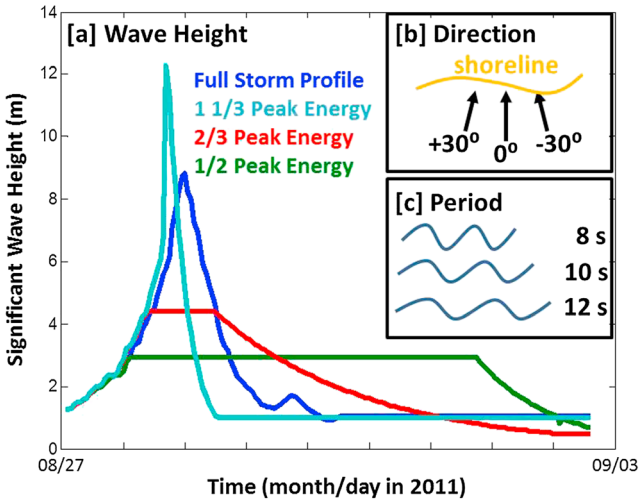

Figure 5. Boundary conditions for storm intensity simulations, including (a) significant wave height, (b) wave direction, and (c) wave period. The energy under each curve of significant wave height versus time (Figure 5a) is identical to that measured during Hurricane Irene (dark blue curve), but distributed differently over time either to enhance the maximum (peak) energy (1 1/3 times, light blue curve) or to decrease peak energy either to 2/3 (red) or 1/2 (green) of the original value. Offshore wave boundary conditions were a JONSWAP spectral shape with a $\cos^{20}\theta$ directional distribution, with wave height given by the time series in Figure 5a and coupled with a mean period and direction that were constant for each 6-day model simulation. Simulations were run for different wave directions (Figure 5b) and wave periods (Figure 5c) that are similar to those observed.

Simulations with no wave energy (not shown) suggest that the waves during Hurricane Irene increased erosion around the inlet by as much as 25% relative to simulations with tidal currents alone. Previous studies indicate that this percentage will increase with higher-energy storms (Luijendijk et al., 2017). In the idealized simulations with a range of storm durations (Figure 6a) and maximum wave heights (Figure 6b), erosion increases with higher storm intensity (R^2= 0.60), even for identical amounts of wave energy entering the model domain (Figure 6c). Thus, hurricanes (shorter duration, higher maximum wave height storms) move more sand at Katama than nor'easters (longer duration, lower maximum wave height storms) with similar overall energy. Erosion decreases as storms become longer, but with lower peak waves (Figure 6a), and erosion increases with maximum significant wave height (Figure 6b), as expected in wave-dominated environments for the formulation used here (Van Rijn, 1993), which combines transport owing to waves (proportional to wave energy) with that owing to tidal currents (proportional to velocity cubed). Katama is a mixed wave-and-tidal-current energy environment, and thus, these results suggest that in addition to tidal-current-driven sediment transport, wave-driven transport is important during storms, with more intense storms moving more sediment.

The trend of bathymetric change (here erosion, although results are similar for deposition and for variance in bathymetric change) with storm intensity is consistent with observations at the Sand Engine in the Netherlands (Luijendijk et al., 2017). Sand Engine observations included storms of varying offshore energy that eroded the

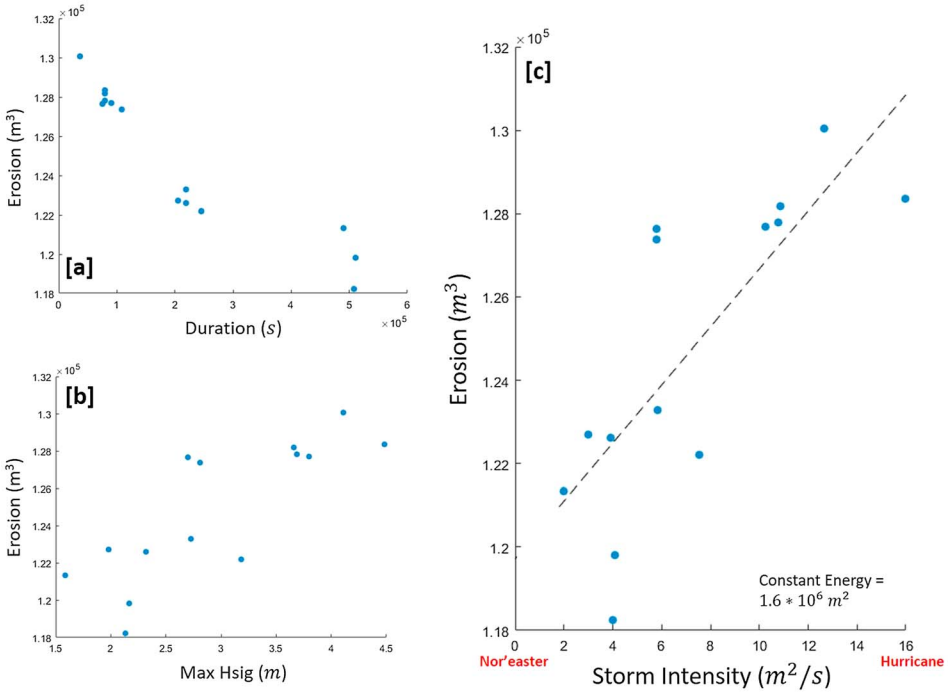

Figure 6. Erosion integrated around the inlet (pink box in Figure 1) versus (a) storm duration, (b) maximum storm significant wave height, and (c) storm intensity. The dashed line in (c), which is the least squares fit between erosion and storm intensity (R^2= 0.60), is not extended to the *x* axis because 0 intensity is not defined for these simulations with constant storm energy (1.6×10^6 m^2).

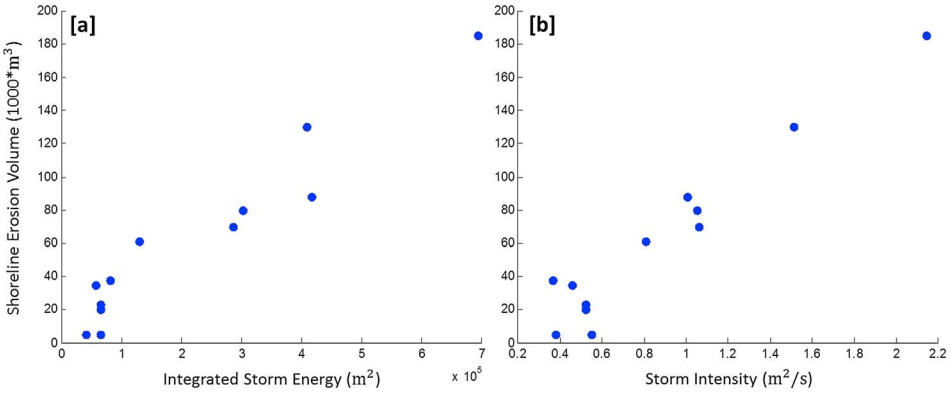

Figure 7. Shoreline erosion volume at the Sand Engine in the Netherlands versus (a) integrated wave energy (R^2 = 0.93) and (b) storm intensity (integrated wave energy divided by storm duration, R^2 = 0.94). Figure 7a and data for Figure 7b are from Luijendijk et al. (2017), with permission.

nourishment in an environment where wave-driven nearshore currents usually are greater than the local tidal currents. The eroded volume is correlated with the integrated storm energy (Figure 7a; Luijendijk et al., 2017). When the integrated energy of the storms is transformed into intensity by dividing by the storm duration, observations at the Sand Engine also suggest that there is a linear relationship between storm intensity and sediment transport if there is sufficient sediment supply (Figure 7). Despite different relative roles of wave- and current-driven transport, the similarity of the relationship between bathymetric change and storm intensity at dissimilar nearshore environments (cf. Figure 6c with Figure 7b) suggests that the temporal distribution of wave energy during storms can impact bathymetric change in a range of mixed wave-and-current energy environments.

5. Conclusion

Numerical simulations (SWAN and Delft3D-FLOW) of hydrodynamics and morphological evolution on the sandy southern shoreline of Martha's Vineyard, MA, near the migrating Katama Inlet during Hurricanes Irene and Sandy are consistent with measured waves, currents, and bathymetric change. Model results show that on time scales of days to weeks, bathymetric change (e.g., erosion and accretion) increases with increasing storm intensity (the total wave energy of the storm divided by the duration of the storm). Thus, the observations and simulations suggest that both total wave energy integrated over the storm duration and storm intensity can influence morphological evolution of a sandy beach system (in this case, the migration of an inlet). In the mixed wave-and-tidal-current energy system investigated here, storms can increase erosion and deposition by 25% more than with tidal current alone, with short, intense storms (e.g., hurricanes) causing more sediment transport than longer, less intense storms (e.g., nor'easters) with the same time-integrated wave energy.

Appendix A
A1. Metrics for Validation

Similar to other 2DH numerical morphological studies (Daly et al., 2014; Ganju et al., 2009, 2011; Luijendijk et al., 2017; Ranasinghe et al., 2011), the Brier Skill Score (BSS) is used to compare the relative skill of different simulations. The skill score is defined in discrete form as

$$\mathrm{BSS} = 1 - \frac{\Sigma(\Delta z_o - \Delta z_m)}{\Sigma(\Delta z_o)}$$

where Δz_o is the observed and Δz_m is the modeled bathymetric change. A BSS = 1 indicates perfect model skill. A BSS < 1 indicates the simulated morphological evolution diverges from the observations. The score can be used to examine in more detail how model and data disagree (or not) as follows (Sutherland et al., 2004)

$$\mathrm{BSS} = \frac{\alpha - \beta - \gamma + \epsilon}{1 + \epsilon}$$

$$\alpha = \left(\frac{\mathrm{cov}(\Delta z_o, \Delta z_m)}{\sigma_{\Delta z_o} \sigma_{\Delta z_m}} \right)^2$$

$$\beta = \left(\sqrt{\alpha} - \frac{\sigma_{\Delta z_m}}{\sigma_{\Delta z_o}} \right)^2$$

$$\gamma = \left(\frac{\Delta z_m - \Delta z_o}{\sigma_{\Delta z_o}} \right)^2$$

$$\epsilon = \left(\frac{\Delta z_o}{\sigma_{\Delta z_o}} \right)^2$$

where σ is the standard deviation, cov is the covariance, and $< >$ is an averaging operator. The term α indicates how well the model simulates the location of bathymetric changes ($\alpha = 1$ is perfect agreement), β indicates how well the model simulates the volume of sand moved ($\beta = 0$ is perfect), γ indicates how well the model simulates the average bed level ($\gamma = 0$ is perfect), and ϵ is a normalization term. Both forms of the BSS are used here to compare numerical simulations with observations of bathymetric change during Hurricanes Irene and Sandy.

A2. Irene and Sandy

Model skill, according to the BSS, is higher for Hurricane Irene than Sandy, but relatively low for each compared with an ideal BSS (*excellent* is classified as a BSS > 0.5, *good* is a BSS > 0.2, and *fair* BSS > 0.1; Luijendijk et al., 2017). Although the simulated bathymetric change is qualitatively consistent with the observed changes (Figures 3 and 4), the best BSS for these runs fall into either the good or fair category. Some of the error could be owing to the (not modeled) morphological evolution that occurred during the times between the bathymetric surveys and the periods around the storms that were simulated. Errors also could be owing to simplifications of model parameters, including assuming a spatially uniform grain size distribution, using a crude parameterization of bottom roughness, and initialization on the outer boundary with simulated wave conditions from WW3.

Breaking the BSS into its components for each model run reveals that most of the error is in the α term, or the spatial discrepancies between model and data (Figures A1 and A2). Some of the location errors may be related to generating the model initial bathymetry by stretching the observed prestorm bathymetry (surveyed in a relatively small area near the inlet) to mesh smoothly with the large-scale bathymetry (before interpolating onto the 13-m grid). As a result, the model bathymetry (and the simulated bathymetric change) was distorted slightly in space relative to the surveyed bathymetry (and bathymetric change), possibly leading to errors in the skill score. The higher model skill for Hurricane Irene than for Hurricane Sandy may be because the spatial shift arising from putting the observed bathymetry on the model grid was reduced by the 60% larger spatial extent of the Hurricane Irene bathymetric surveys.

Additionally, the peak of each storm occurred at different phases of the tidal cycle, which could impact the response to the storm-force waves. However, overall bathymetric evolution during the storms did not change significantly if the time series of waves on the boundary was shifted 6 hr, suggesting that storm timing did not have a significant impact.

A3. Boundary Condition Calibration

Standard boundary conditions for model runs included waves (from a buoy in 50-m water depth or from WW3 model output) and satellite-derived tidal constituents (Egbert & Erofeeva, 2002). Optional boundary conditions include wind and atmospheric pressure during storms. Observed winds were spatially sparse (with only one station on Martha's Vineyard and one station on Nantucket Island for the entire model domain), so WW3 winds were used in the model with the simulated wave conditions verified with

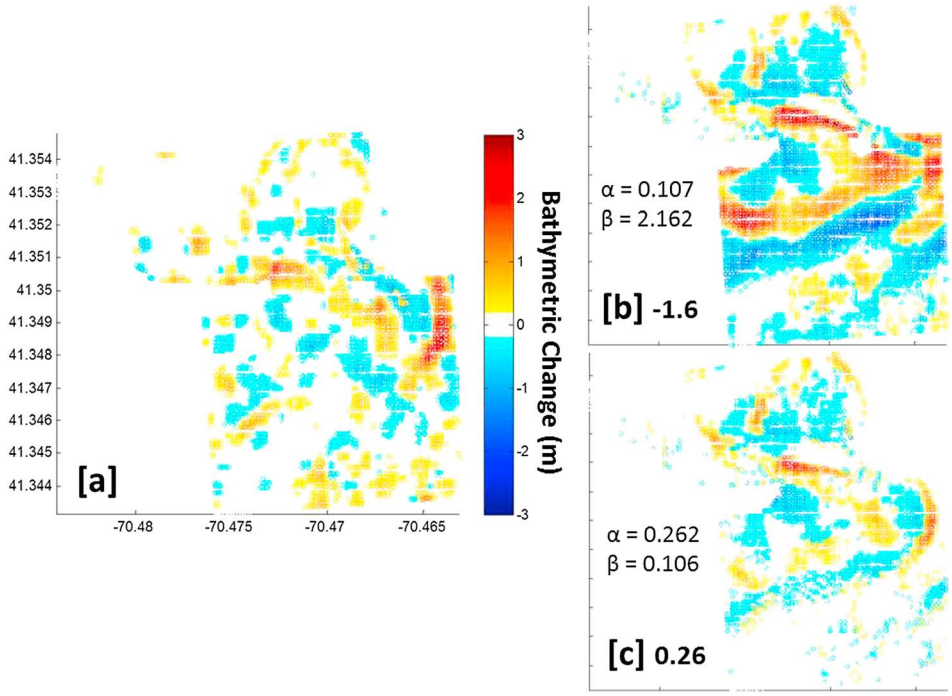

Figure A1. Contours of bathymetric change (red = accretion, blue = erosion, scale on the right in (a)) owing to Hurricane Irene for (a) observations, (b) model simulations without wind, and (c) model simulations with wind. The Brier Skill Score is indicated in bold (lower left) in (b) and (c), along with the components of the skill score above (α = location error and β = magnitude error).

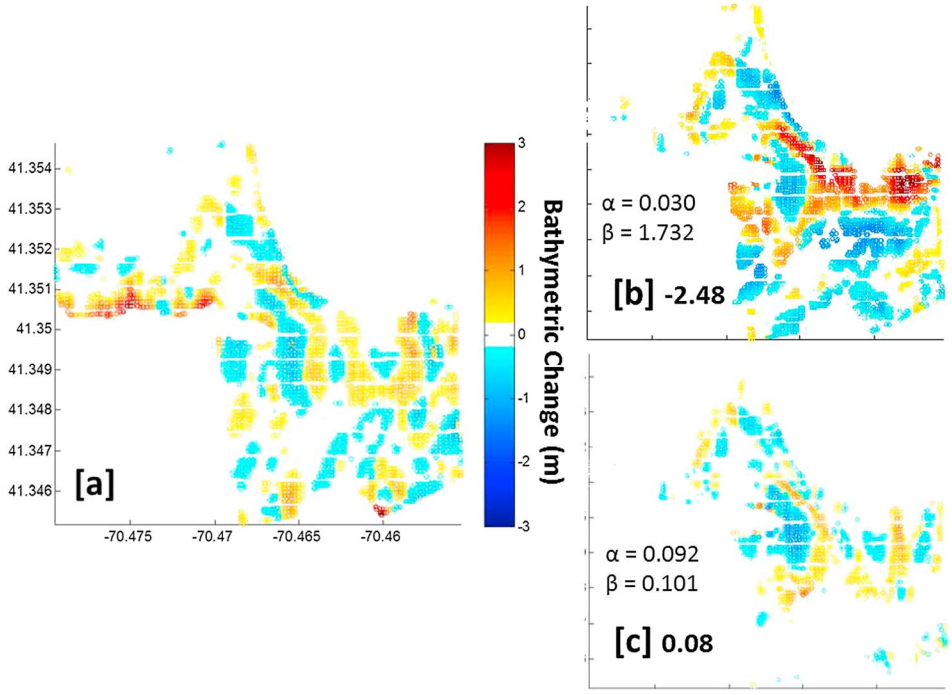

Figure A2. Contours of bathymetric change (red = accretion, blue = erosion, scale on the right in (a)) owing to Hurricane Sandy for (a) observations, (b) model simulations without wind, and (c) model simulations with wind. The Brier Skill Score is indicated in bold (lower left) in (b) and (c), along with the components of the skill score above (α = location error and β = magnitude error).

observations. Wind coefficients in the model were left at default values. Similarly, WW3 pressure fields were used in model simulations.

Simulated bathymetric changes for Hurricanes Irene and Sandy show significantly greater skill with the inclusion of wind than without wind (cf. Figure A1b with Figure A1c and Figure A2b with Figure A2c). Including spatially varying atmospheric pressure did not result in significant improvement in model skill (not shown). To save computational costs, neither wind nor pressure were included in the idealized model runs, which did not simulate a specific observed morphological change.

Acknowledgments
The best method to obtain the data used in this study and to ensure notification of quality control updates is to contact Steve Elgar (elgar@whoi.edu) or Britt Raubenheimer (britt@whoi.edu). Alternatively, the data can be accessed here: https://pv-lab.org/katama/. We thank the PVLAB field team, and especially Levi Gorrell for deploying, maintaining, and recovering sensors and for obtaining bathymetric surveys in less than ideal conditions for many years, Chris Kennedy of the Trustees of Reservations for valuable discussions about the Martha's Vineyard shoreline and for logistical help, Neil Ganju for helpful comments and suggestions, and Paul Bagnold and the Martha's Vineyard shell fishermen for their advice and help in the shallow shoals of Katama Bay. Funding was provided by the National Science Foundation, the National Oceanic and Atmospheric Administration Sea Grant, National-Security-Science-and-Engineering and Vannevar-Bush Faculty Fellowships, both from the Assistant Secretary of Defense (Research and Engineering), and a National Defense Science and Engineering Graduate award.

References

Anderson, D. (2012). Sediment transport processes in a coastal lagoon: Katama Bay, Martha's Vineyard. Bachelor's Thesis, BU. Boston University.

Avila, L. A., & Cangialosi, J. (2011). Tropical cyclone report: Hurricane Irene (Rep. AL092011). *National Hurricane Center*. Miami, FL. Retrieved from http://www.nhc.noaa.gov/data/tcr/AL092011_Irene.pdf

Battjes, J. A., & Janssen, J. P. F. M. (1978). Energy loss and set-up due to breaking of random waves. In *International Conference on Coastal Engineering* (pp. 569–587).

Blake, E. S., Kimberlain, T. B., Cangialosi, J. P., & Beven II, J. L. (2013). Tropical cyclone report: Hurricane Sandy (Rep. *AL182012)*. *National Hurricane Center*. Miami, FL. Retrieved from http://www.nhc.noaa.gov/data/tcr/AL182012_Sandy.pdf

Booij, N., Ris, R. C., & Holthuijsen, L. H. (1999). A third-generation wave model for coastal regions: 1. Model description and validation. *Journal of Geophysical Research*, *104*(C4), 7649. https://doi.org/10.1029/98JC02622

Daly, C. J., Bryan, K. R., Gonzalez, M. R., Klein, A. H. F., & Winter, C. (2014). Effect of selection and sequencing of representative wave conditions on process-based predictions of equilibrium embayed beach morphology. *Ocean Dynamics*, *64*(6), 863–877. https://doi.org/10.1007/s10236-014-0730-9

Dean, R. G., & Dalrymple, R. A. (1991). *Water wave mechanics for engineers and scientists* (Vol. 2). London: World Scientific. https://doi.org/10.1142/1232

Deltares (2014). Delft3D-Wave. Simulation of short crested waves with SWAN. User manual. Deltares, Rotterdamseweg 185, The Netherlands.

Dietrich, J. C., Tanaka, S., Westerink, J. J., Dawson, C. N., Luettich, R. A., Zijlema, M., et al. (2011). Performance of the unstructured-mesh, SWAN +ADCIRC model in computing hurricane waves and surge. *Journal of Scientific Computing*, *52*(2), 468–497. https://doi.org/10.1007/s10915-011-9555-6

Dissanayake, P., Brown, J., & Karunarathna, H. (2014). Modelling storm-induced beach/dune evolution: Sefton coast, Liverpool Bay, UK. *Marine Geology*, *357*, 225–242. https://doi.org/10.1016/j.margeo.2014.07.013

Eakins, B. W., Taylor, L. A., Carignan, K. S., Warnken, R. R., Lim, E., & Medley, P. R. (2009). *Digital Elevation Model of Nantucket, Massachusetts: Procedures, data sources and analysis, NOAA Technical Memorandum NESDIS NGDC-26* (p. 29). Boulder, CO: Department of Commerce.

Egbert, G. D., & Erofeeva, S. Y. (2002). Efficient inverse modeling of barotropic ocean tides. *Journal of Atmospheric and Oceanic Technology*, *19*, 183–204.

Ganju, N. K., Jaffe, B. E., & Schoellhamer, D. H. (2011). Discontinuous hindcast simulations of estuarine bathymetric change: A case study from Suisun Bay, California. *Estuarine, Coastal and Shelf Science*, *93*(2), 142–150. https://doi.org/10.1016/j.ecss.2011.04.004

Ganju, N. K., Schoellhamer, D. H., & Jaffe, B. E. (2009). Hindcasting of decadal-timescale estuarine bathymetric change with a tidal-timescale model. *Journal of Geophysical Research*, *114*, F04019. https://doi.org/10.1029/2008JF001191

Hapke, C. J., Plant, N. G., Henderson, R. E., Schwab, W. C., & Nelson, T. R. (2016). Decoupling processes and scales of shoreline morphodynamics. *Marine Geology*, *381*, 42–53. https://doi.org/10.1016/j.margeo.2016.08.008

Harter, C., & Figlus, J. (2017). Numerical modeling of the morphodynamic response of a low-lying barrier island beach and foredune system inundated during Hurricane Ike using XBeach and CSHORE. *Coastal Engineering*, *120*(April 2016), 64–74. https://doi.org/10.1016/j.coastaleng.2016.11.005

Herrling, G., & Winter, C. (2014). Morphological and sedimentological response of a mixed-energy barrier island tidal inlet to storm and fair-weather conditions. *Earth Surface Dynamics*, *2*(1), 363–382. https://doi.org/10.5194/esurf-2-363-2014

Hopkins, J., Elgar, S., & Raubenheimer, B. (2016). Observations and model simulations of wave-current interaction on the inner shelf. *Journal of Geophysical Research: Oceans*, *121*, 198–208. https://doi.org/10.1002/2015JC010788

Hopkins, J., Elgar, S., & Raubenheimer, B. (2017). Flow separation effects on shoreline sediment transport. *Coastal Engineering*, *125*, 23–27. https://doi.org/10.1016/j.coastaleng.2017.04.007

Kaji, A., Luijendijk, A. P., van Thiel de Vries, J. S. M., de Schipper, M. A., & Stive, M. J. F. (2014). Effect of different forcing processes on the longshore sediment transport at the sand motor, the Netherlands. *Coastal Engineering Proceedings*, *1*, 1–11. https://doi.org/10.9753/icce.v34.sediment.71

Lesser, G. R., Roelvink, J. A., & van Kester, J. a. T. M., & Stelling, G. S. (2004). Development and validation of a three-dimensional morphological model. *Coastal Engineering*, *51*, 883–915. https://doi.org/10.1016/j.coastaleng.2004.07.014

Lindemer, C. A., Plant, N. G., Puleo, J. A., Thompson, D. M., & Wamsley, T. V. (2010). Numerical simulation of a low-lying barrier island's morphological response to Hurricane Katrina. *Coastal Engineering*, *57*(11–12), 985–995. https://doi.org/10.1016/j.coastaleng.2010.06.004

Luijendijk, A. P., Ranasinghe, R., de Schipper, M. A., Huisman, B. A., Swinkels, C. M., Walstra, D. J. R., & Stive, M. J. F. (2017). The initial morphological response of the Sand Engine: A process-based modelling study. *Coastal Engineering*, *119*, 1–14. https://doi.org/10.1016/j.coastaleng.2016.09.005

Masselink, G., Castelle, B., Scott, T., Dodet, G., Suanez, S., Jackson, D., & Floc'h, F. (2016). Extreme wave activity during 2013/2014 winter and morphological impacts along the Atlantic coast of Europe. *Geophysical Research Letters*, *43*, 2135–2143. https://doi.org/10.1002/2015GL067492

Miller, H. C. (1999). Field measurements of longshore sediment transport during storms. *Coastal Engineering*, *36*(4), 301–321. https://doi.org/10.1016/S0378-3839(99)00010-1

Moore, L. J., McNamara, D. E., Murray, A. B., & Brenner, O. (2013). Observed changes in hurricane-driven waves explain the dynamics of modern cuspate shorelines. *Geophysical Research Letters*, *40*, 5867–5871. https://doi.org/10.1002/2013GL057311

Morton, R. A., Gibeaut, J. C., & Paine, J. G. (1995). Meso-scale transfer of sand during and after storms: implications for prediction of shoreline movement. *Marine Geology*, *126*(1–4), 161–179. https://doi.org/10.1016/0025-3227(95)00071-6

Mulligan, R. P., Hay, A. E., & Bowen, A. J. (2010). A wave-driven jet over a rocky shoal. *Journal of Geophysical Research*, *115*, C10038. https://doi.org/10.1029/2009JC006027

National Geophysical Data Center (1999). *U.S. coastal relief model–Northeast Atlantic*. Boulder, CO: National Oceanic and Atmos. Admin. https://doi.org/10.7289/V5MS3QNZ

Orescanin, M. M., Elgar, S., & Raubenheimer, B. (2016). Changes in bay circulation in an evolving multiple inlet system. *Continental Shelf Research*, *124*, 13–22. https://doi.org/10.1016/j.csr.2016.05.005

Radermacher, M., de Schipper, M. A., Swinkels, C., MacMahan, J. H., & Reniers, A. J. H. M. (2017). Tidal flow separation at protruding beach nourishments. *Journal of Geophysical Research: Oceans*, *122*, 63–79. https://doi.org/10.1002/2016JC011942

Ranasinghe, R., Swinkels, C., Luijendijk, A., Roelvink, D., Bosboom, J., Stive, M., & Walstra, D. (2011). Morphodynamic upscaling with the MORFAC approach: Dependencies and sensitivities. *Coastal Engineering*, *58*(8), 806–811. https://doi.org/10.1016/j.coastaleng.2011.03.010

Ruggiero, P., Buijsman, M., Kaminsky, G. M., & Gelfenbaum, G. (2010). Modeling the effects of wave climate and sediment supply variability on large-scale shoreline change. *Marine Geology*, *273*(1–4), 127–140. https://doi.org/10.1016/j.margeo.2010.02.008

Smallegan, S. M., Irish, J. L., Van Dongeren, A. R., & Den Bieman, J. P. (2016). Morphological response of a sandy barrier island with a buried seawall during Hurricane Sandy. *Coastal Engineering*, *110*, 102–110. https://doi.org/10.1016/j.coastaleng.2016.01.005

Sutherland, J., Peet, A. H., & Soulsby, R. L. (2004). Evaluating the performance of morphological models. *Coastal Engineering*, *51*(8–9), 917–939. https://doi.org/10.1016/j.coastaleng.2004.07.015

Tolman, H. L. (2002). User manual and system documentation of WAVEWATCH-III version 2.22. *NOAA/NWS/NCEP/MMAB Technical Note*, *222*, 133.

Van Rijn, L. (1993). *Principles of sediment transport in rivers, estuaries and coastal seas*. Blokzijl, Netherlands: Aqua Publishing.

Wahl, T., & Plant, N. G. (2015). Changes in erosion and flooding risk due to long-term and cyclic oceanographic trends. *Geophysical Research Letters*, *42*, 2943–2950. https://doi.org/10.1002/2015GL063876

Walstra, D.-J., De Vroeg, J., Van Thiel de Vries, J., Swinkels, C., Luijendijk, A., De Boer, W., & Godsey, E. (2012). A comprehensive sediment budget for the Mississippi Barrier Islands. *Coastal Engineering Proceedings*, *1*(33), 81. https://doi.org/10.9753/icce.v33.sediment.81

Walstra, D. J. R., Hoekstra, R., Tonnon, P. K., & Ruessink, B. G. (2013). Input reduction for long-term morphodynamic simulations in wave-dominated coastal settings. *Coastal Engineering*, *77*, 57–70. https://doi.org/10.1016/j.coastaleng.2013.02.001